

AD-A039 643

AEROSPACE CORP EL SEGUNDO CALIF CHEMISTRY AND PHYSICS LAB F/G 7/4
CLASSICAL TRAJECTORY STUDY OF THE EFFECT OF VIBRATIONAL ENERGY --ETC(U)
APR 77 B R JOHNSON, N A WINTER F04701-76-C-0077

UNCLASSIFIED

TR-0077(2970)-1

SAMSO-TR-77-77

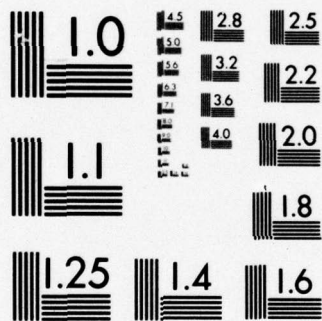
NL

| OF |
AD
A039643



END

DATE
FILMED
6-77



MICROCOPY RESOLUTION TEST CHART
NATIONAL BUREAU OF STANDARDS-1963-A

AD A 039643

**Classical Trajectory Study of the Effect of
Vibrational Energy on the Reaction of
Molecular Hydrogen with Atomic Oxygen**

Chemistry and Physics Laboratory
The Ivan A. Getting Laboratories
The Aerospace Corporation
El Segundo, Calif. 90245

and

Lawrence Livermore Laboratory
University of California
Livermore, Calif. 94550

15 April 1977

Interim Report

APPROVED FOR PUBLIC RELEASE:
DISTRIBUTION UNLIMITED

Prepared for

SPACE AND MISSILE SYSTEMS ORGANIZATION
AIR FORCE SYSTEMS COMMAND
Los Angeles Air Force Station
P.O. Box 92960, Worldway Postal Center
Los Angeles, Calif. 90009

AD No. _____
DDC FILE COPY



This interim report was submitted by The Aerospace Corporation, El Segundo, CA 90245, under Contract No. F04701-76-C-0077 with the Space and Missile Systems Organization, Deputy for Advanced Space Programs, P. O. Box 92960, Worldway Postal Center, Los Angeles, CA 90009. It was reviewed and approved for The Aerospace Corporation by S. Siegel, Director, Chemistry and Physics Laboratory. Lieutenant Dara Batki, SAMSO/YAPT, was the project officer for Advanced Space Programs.

This report has been reviewed by the Information Office (OI) and is releasable to the National Technical Information Service (NTIS). At NTIS, it will be available to the general public, including foreign nations.

This technical report has been reviewed and is approved for publication.

Dara Batki
Dara Batki, Lt. USAF
Project Officer

J. Gassmann
Joseph Gassmann, Major, USAF

FOR THE COMMANDER

Floyd R. Stuart
Floyd R. Stuart, Colonel, USAF
Deputy for Advanced Space Programs

UNCLASSIFIED

SECURITY CLASSIFICATION OF THIS PAGE (When Data Entered)

19 REPORT DOCUMENTATION PAGE		READ INSTRUCTIONS BEFORE COMPLETING FORM
1. REPORT NUMBER 18 SAMSO-TR-77-77	2. GOVT ACCESSION NO.	3. REPORT'S CATALOG NUMBER 9
4. TITLE (and Subtitle) 6 CLASSICAL TRAJECTORY STUDY OF THE EFFECT OF VIBRATIONAL ENERGY ON THE REACTION OF MOLECULAR HYDROGEN WITH ATOMIC OXYGEN.	5. TYPE OF REPORT & PERIOD COVERED Interim / rept.	
7. AUTHOR(s) 10 Bernard R. Johnson (The Aerospace Corporation) and Nicholas A. Winter (Lawrence Livermore Laboratory)	14. PERFORMING ORG. REPORT NUMBER TR-0077(2970)-1	
9. PERFORMING ORGANIZATION NAME AND ADDRESS The Aerospace Corporation El Segundo, Calif. 90245	15. CONTRACT OR GRANT NUMBER(s) F04701-76-C-0077	
11. CONTROLLING OFFICE NAME AND ADDRESS Space and Missile Systems Organization Air Force Systems Command Los Angeles, Calif. 90009	12. REPORT DATE 11 15 Apr 1977	
14. MONITORING AGENCY NAME & ADDRESS (if different from Controlling Office) 12 26p.	13. NUMBER OF PAGES 24	
16. DISTRIBUTION STATEMENT (of this Report) Approved for public release; distribution unlimited	15. SECURITY CLASS. (of this report) Unclassified	
17. DISTRIBUTION STATEMENT (of the abstract entered in Block 20, if different from Report)	15a. DECLASSIFICATION/DOWNGRADING SCHEDULE	
18. SUPPLEMENTARY NOTES		
19. KEY WORDS (Continue on reverse side if necessary and identify by block number) Classical Trajectory Reactive Collision Molecular Hydrogen Monte Carlo Reaction Rate		
20. ABSTRACT (Continue on reverse side if necessary and identify by block number) The dynamics of the reaction $O + H_2(v) \rightarrow OH + H$ is studied by means of three dimensional classical trajectory calculations on an LEPS potential energy surface. Rate constants are calculated for the two cases in which the H_2 molecule is initially in the $v = 0$ and $v = 1$ vibrational state. In the temperature range 298-1000 K these rates are fit very well by the formulas ($cm^3 \text{ molecule}^{-1} \text{ sec}^{-1}$) $k = 2.81T \times 10^{-14} \exp(-4279/T)$ and $k^\dagger = 4.65 T \times 10^{-14} \exp(-1868/T)$. The calculated value of k^\dagger at 300°K is $2.8 \times 10^{-14} \text{ cm}^3 \text{ molecule}^{-1} \text{ sec}^{-1}$, which is below		

DD FORM 1473
(FACSIMILE)

409383

UNCLASSIFIED
SECURITY CLASSIFICATION OF THIS PAGE (When Data Entered)DDC
RECEIVED
MAY 19 1977
MILITARY

UNCLASSIFIED

SECURITY CLASSIFICATION OF THIS PAGE(When Data Entered)

19. KEY WORDS (Continued)

20. ABSTRACT (Continued)

the upper bound established by Birely et al. The branching ratio Γ , defined as the ratio of the rates for populating the $v' = 1$ and $v' = 0$ state of OH when H_2 is initially in the $v = 1$ state, is also calculated and fit by the expression $\Gamma = 2.3 \exp(196/T)$. The value at 300°K is 4.4.

ADDITIONAL

NTIS	White Section	<input checked="" type="checkbox"/>
DOC	Buff Section	<input type="checkbox"/>
UNANNOUNCED		<input type="checkbox"/>
JUSTIFICATION.....		
BY.....		
DISTRIBUTION/AVAILABILITY CODES		
Dist.	AVAIL. and/or SPECIAL	
A		

UNCLASSIFIED

SECURITY CLASSIFICATION OF THIS PAGE(When Data Entered)

Preface

We wish to acknowledge useful discussions of this problem with J. H. Birely, G. C. Light, L. R. Martin and R. R. Herm. We also thank Ms. J. Frawley for programming assistance and J. M. Bowman and L. C. Leasure for a preprint of their paper.

CONTENTS

PREFACE.....	1
I. INTRODUCTION.....	9
II. POTENTIAL ENERGY SURFACE	9
III. COMPUTATIONAL PROCEDURE	10
IV. RESULTS AND DISCUSSION.....	15
REFERENCES.....	25

FIGURES

1.	Contour map of the LEPS potential energy surface for the O + H ₂ system in the colinear configuration	12
2.	Schematic diagram of the energy along the minimum energy path on the potential surface shown in Figure 1	13
3.	A plot of the reactive cross sections $\sigma(v, J; E)$	17
4.	Rate constants, $k(v, T)$, for the reaction O + H ₂ (v) → OH + H where v is the vibrational quantum number of H ₂	22

TABLES

I.	Potential Parameters Used in the LEPS Surface for the O-H _a -H _b System	11
II.	Coefficients and Threshold Energies for $\sigma(v, J; E)$	16
III.	Computed Results at Selected Temperatures	19

I. INTRODUCTION

The influence of reagent vibrational energy on the rate of chemical reactions is the subject of a great deal of interest.¹⁻⁸ It is of special importance to laser enhanced reactions,³⁻⁶ atmospheric reactions under disturbed conditions and combustion processes in general. Recent studies⁴⁻⁸ have demonstrated rate accelerations of several orders of magnitude when one of the collision partners is vibrationally excited. The reaction $O + H_2^{\uparrow}(v=1) \xrightarrow{\text{goes to}} OH + H$ has recently received attention because of its importance in modeling IR radiation in certain rocket plumes. Birely et al.¹ have set an experimental upper bound on the rate for this reaction, and Light⁹ is currently measuring the actual rate.

We report here the results^{are reported} of an extensive classical trajectory study of the reaction of atomic oxygen with both $H_2^{\uparrow}(v=0)$ and $H_2^{\uparrow}(v=1)$ using an LEPS potential energy surface. In addition to determining the rates for these reactions, ~~we have calculated~~ the branching ratio is calculated for the production of $OH(v'=1)$ and $OH(v'=0)$ when $H_2^{\uparrow}(v=1)$ is the reactant.

II. POTENTIAL ENERGY SURFACE

The potential energy surface used in these calculations was an LEPS function¹⁰ with a single adjustable Sato parameter. The Sato parameter was adjusted by trial and error so that the computed rate constant of the reaction $O + H_2 \rightarrow OH + H$ would approximately equal the experimentally observed rate at a particular temperature. We are primarily interested in low temperature results. At 320°K, Campbell and Thrush¹¹ measured the rate constant to be $k = (2.0 \pm 0.16) \times 10^{-17} \text{ cm}^3 \text{ molecule}^{-1} \text{ sec}^{-1}$. In a very recent set of low temperature measurements from 347 to 742°K, Dubinsky and McKenney¹² state that their results extrapolate to within 11 percent of the Campbell and Thrush value. The actual extrapolated value, using their Arrhenius parameters, is $k = 1.77 \times 10^{-17} \text{ cm}^3 \text{ molecule}^{-1} \text{ sec}^{-1}$. The value of k calculated from the Leeds formula¹³ at this temperature is $k = 0.8 \times 10^{-17} \text{ cm}^3$

molecule⁻¹ sec⁻¹. This is probably too low, while the Campbell and Thrush point may be somewhat high. The value of the Sato parameter, adjusted to make the calculated k fall somewhere between these limits, is $\Delta = 0.0885$. The calculated rate constant, using this value, is $k = 1.4 \times 10^{-17}$ cm³ molecule⁻¹ sec⁻¹. This rate was computed with H₂ in the $v = 0$ state. This is valid, since contributions of the $v = 1$ state to the rate is negligible for temperatures less than 1000 °K.

A complete list of the LEPS potential parameters is given in Table I. A contour plot of this potential for the collinear configuration is shown in Figure 1. The minimum energy path profile is displayed in Figure 2. The reaction barrier along this path is 12.5 kcal/mole with respect to the reactants channel. Also indicated in Figure 2 are the energies for the zeroth and first vibrational levels of both products and reactants. The barrier height is significantly above the experimental activation of 8.9 kcal/mole. Of course by adjusting the surface to reproduce the experimental rate, we have, to some extent, incorporated the effects of zero point energy differences and tunneling into our semiempirical surface.

III. COMPUTATIONAL PROCEDURE

A slightly modified version of Muckerman's classical trajectory program CLASTR¹⁴ was used to compute the state-to-state reactive cross sections. The modification we made consisted of changing the method of choosing the impact parameters. Following a suggestion of Porter,¹⁷ the values of the impact parameter, b , were restricted to the discrete set that corresponds to integral values of the orbital angular momentum quantum number l . Accordingly,

$$b_l = \hbar(2\mu E)^{-1/2} (l + 1/2), \quad (1)$$

where μ is the reduced mass of the system and E is the initial relative translational energy. The state-to-state reactive cross section is then given by

Table I
Potential Parameters Used in the LEPS Surface for the $\text{O-H}_a\text{-H}_b$ System

Parameter	O-H_a	$\text{H}_a\text{-H}_b$	O-H_b
β (\AA^{-1})	2.294	1.942	2.294
D_e (kcal/mole)	106.6	109.4	106.6
r_0 (\AA)	0.9706	0.7417	0.9706
Δ	0.0885	0.0885	0.0885

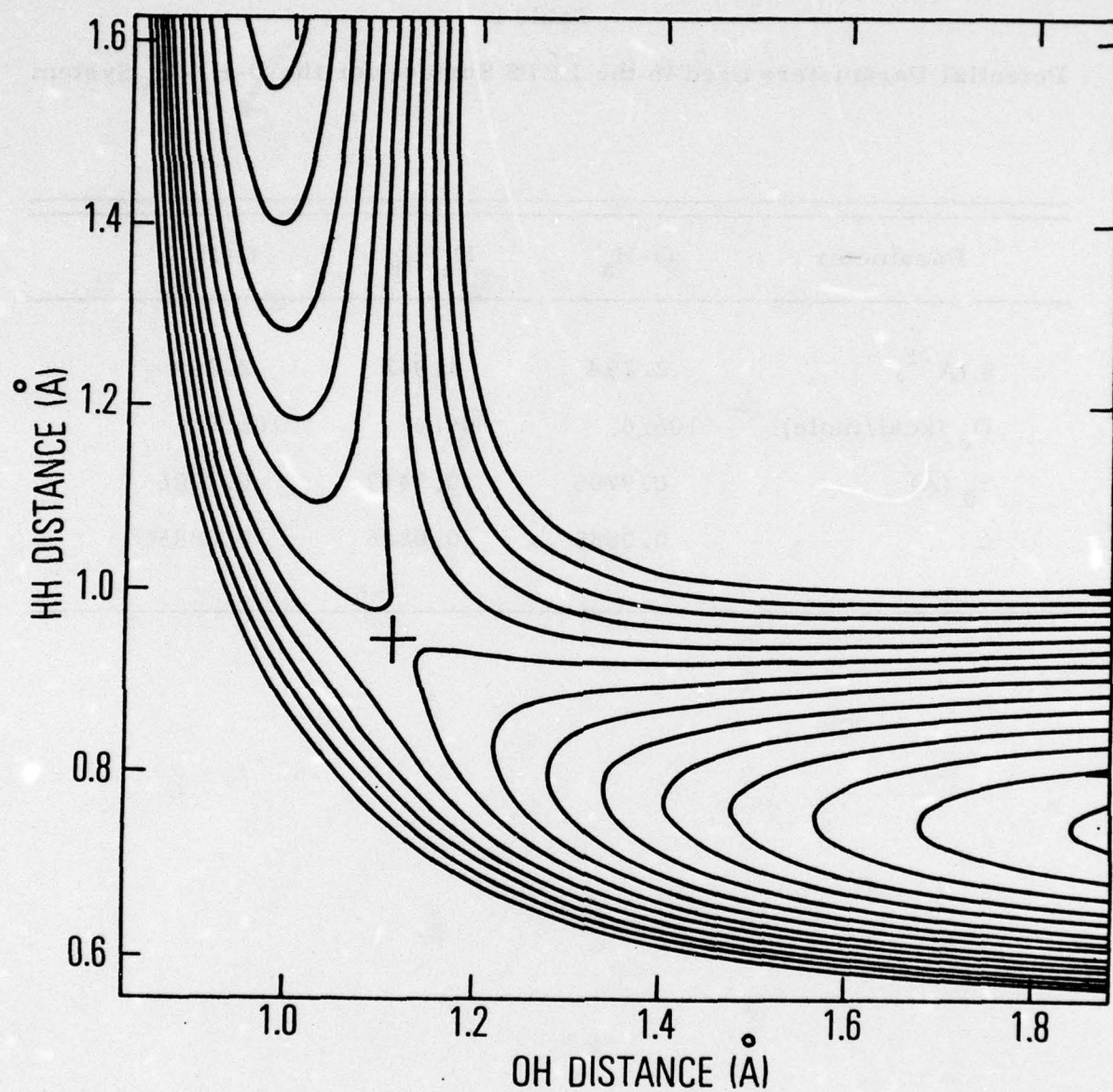


Figure 1. Contour map of the LEPS potential energy surface for the $O + H_2$ system in the colinear configuration. The saddle point marked by the symbol + occurs at $O-H = 1.118\text{\AA}$ and $H-H = 0.953\text{\AA}$.

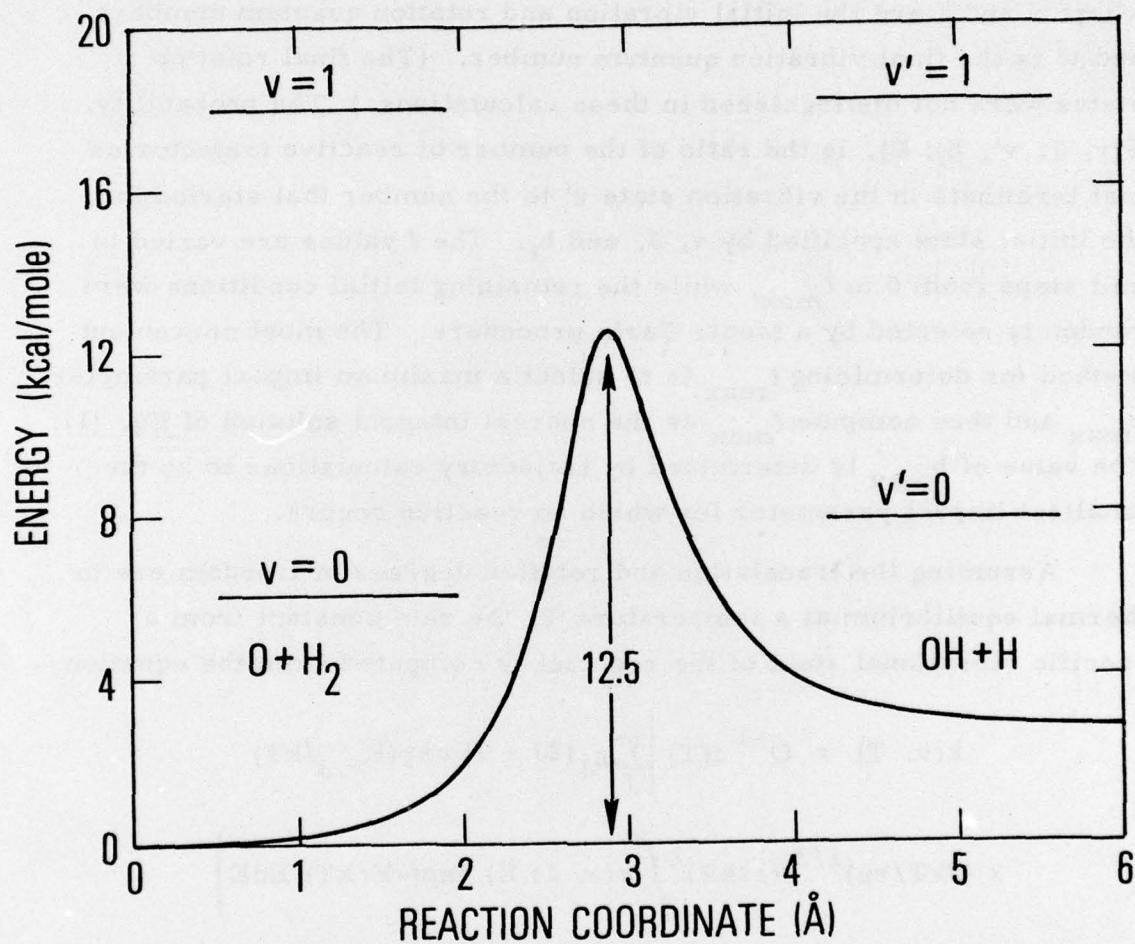


Figure 2. Schematic diagram of the energy along the minimum energy path on the potential surface shown in Figure 1. Also indicated are the energy levels of the zeroth and first vibrational levels of both products and reactants.

$$\sigma_0(v, J, v'; E) = (\pi \hbar^2 / 2\mu E) \sum_{l=0}^{l_{\max}} (2l+1) P(v, J, v', b_l; E) \quad (2)$$

where v and J are the initial vibration and rotation quantum numbers and v' is the final vibration quantum number. (The final rotation states were not distinguished in these calculations.) The probability, $P(v, J, v', b_l; E)$, is the ratio of the number of reactive trajectories that terminate in the vibration state v' to the number that started in the initial state specified by v, J , and b_l . The l values are varied in unit steps from 0 to l_{\max} , while the remaining initial conditions were randomly selected by a Monte Carlo procedure. The most convenient method for determining l_{\max} is to select a maximum impact parameter b_{\max} and then compute l_{\max} as the nearest integral solution of Eq. (1). The value of b_{\max} is determined by trajectory calculations to be the smallest impact parameter for which no reaction occurs.

Assuming the translation and rotation degrees of freedom are in thermal equilibrium at a temperature T , the rate constant from a specific vibrational state of the reactant is computed from the equation

$$k(v, T) = Q^{-1} f(T) \left\{ \sum_J g_J (2J+1) \exp(E_{v,J}/kT) \right. \\ \left. \times (8kT/\pi\mu)^{1/2} (1/kT)^2 \int_0^\infty \sigma(v, J; E) \exp(-E/kT) E dE \right\} \quad (3)$$

where $E_{v,J}$ is the vibration-rotation energy of the reactant molecule, g_J is the statistical weight of the rotation state J (in the case of H_2 , $g_J = 1$ for even J and $g_J = 3$ for odd J), Q is the rotational partition function, $f(T)$ is the probability that the system is initially on an electronic surface on which the reaction can occur (multiple surface coefficient^{18,19}) and $\sigma(v, J; E)$ is the reaction cross section summed over final vibration states

$$\sigma(v, J; E) = \sum_{v'} \sigma_0(v, J, v'; E). \quad (4)$$

In order to carry out the integration in Eq. (3) and also to help average out statistical errors, the computed cross section points are fitted by least squares to the function

$$\sigma(v, J; E) = \begin{cases} 0 & E \leq E_{th}(v, J) \\ \sum_{n=0}^4 A_n(v, J) [E^{-n} - E_{th}^{-n}(v, J)] & E > E_{th}(v, J). \end{cases} \quad (5)$$

This is substituted into Eq. (3) which is then evaluated numerically. The threshold energy, $E_{th}(v, J)$, is determined by fitting a straight line to the lowest few cross section points and extrapolating to zero cross section.

IV. RESULTS AND DISCUSSION

A total of ten reactive cross section curves, $\sigma(v, J; E)$ vs. E , corresponding to the initial quantum numbers $v = 0, 1$ and $J = 0, 1, 2, 3$ and 4 , were computed for the reaction $O + H_2(v, J) \rightarrow OH + H$. About 300 trajectories were calculated for each cross section point. The coefficients $A_n(v, J)$ along with the threshold energies $E_{th}(v, J)$, which when substituted into Eq. (5) provide a good fit to the calculated cross sections, are listed in Table II, and the curves are displayed graphically in Figure 3.

As stated above, $f(T)$ is the probability that the system is initially on an electronic surface that will allow a reaction to occur. The initial state of the reactants is $O(^3P) + H_2(^1\Sigma_g^+)$. If spin-orbit forces are neglected this state is ninefold degenerate and correlates with both $^3\Sigma$ and $^3\Pi$ states of a linear complex. The products $OH(^2\Pi) + H(^2S)$ correlate with $^1\Pi$ and $^3\Pi$ states. Thus, the $^3\Pi$ linear complex, which

Table II
Coefficients and Threshold Energies for $\sigma(v, J; E)^a$

v	J	A_1	A_2	A_3	E_{th}^b
0	0	-122.460	1040.80	-2968.50	8.40
0	1	- 89.974	680.39	-1740.80	8.40
0	2	-157.280	1418.30	-4416.20	8.60
0	3	- 88.781	562.99	-1152.70	7.70
0	4	- 71.766	320.91	- 219.81	8.03
1	0	- 52.308	193.32	- 241.11	3.48
1	1	- 36.404	106.59	- 101.78	3.39
1	2	- 47.882	137.45	- 125.36	3.53
1	3	- 39.533	77.44	- 6.06	3.90
1	4	- 47.327	127.71	- 87.17	4.05

^aThe coefficients A_n in Eq. (5) are such that the units of $\sigma(v, J; E)$ are angstroms² and the unit of energy is kcal/mole.

^bIn units of kcal/mole.

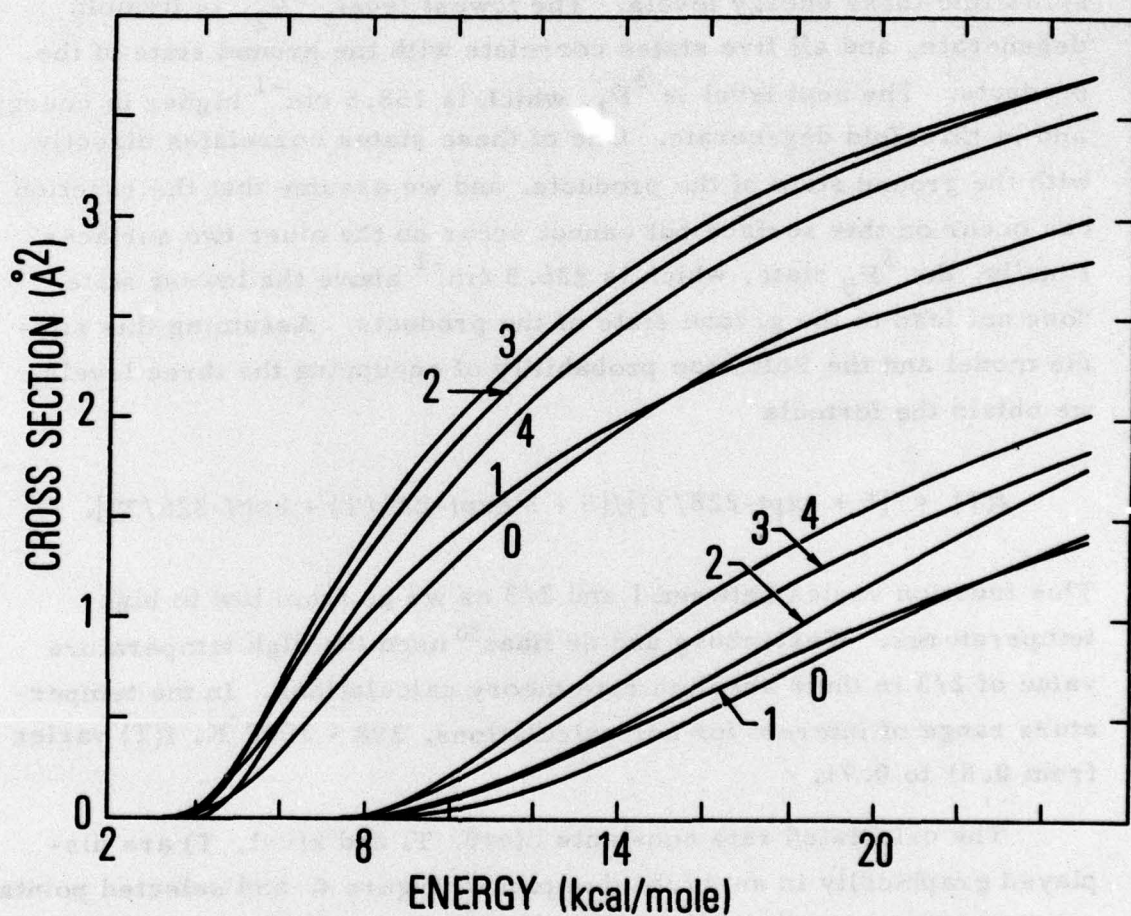


Figure 3. A plot of the reactive cross sections $\sigma(v, J; E)$. The numbers labeling each curve are the rotational quantum number J ; the set of curves with threshold near 4.0 correspond to the vibrational quantum number $v = 1$ and the set with threshold near 8.5 correspond to $v = 0$. These curves are a plot of the analytic fit, i. e., Eq. (5), using the coefficients listed in Table II.

has six states, correlates with both products and reactants. This simple analysis indicates that six of the nine initial states correlate with the products yielding $f(T) = 6/9$. This approximation is adequate at high temperature, but at low temperatures the splitting of the initial state by spin-orbit forces becomes important. The 3P state splits into three energy levels. The lowest level, 3P_2 , is fivefold degenerate, and all five states correlate with the ground state of the products. The next level is 3P_1 , which is 158.5 cm^{-1} higher in energy and is threefold degenerate. One of these states correlates directly with the ground state of the products, and we assume that the reaction can occur on this surface but cannot occur on the other two surfaces. Finally, the 3P_0 state, which is 226.5 cm^{-1} above the lowest state, does not lead to the ground state of the products. Assuming this simple model and the Boltzman probability of occupying the three levels, we obtain the formula

$$f(T) = [5 + \exp(-228/T)]/[5 + 3 \exp(-228/T) + \exp(-326/T)]. \quad (6)$$

This function varies between 1 and 2/3 as we go from low to high temperatures. Westenburg and de Haas²⁰ used the high temperature value of 2/3 in their absolute rate theory calculations. In the temperature range of interest for our calculations, 298 - 1000°K, $f(T)$ varies from 0.81 to 0.71.

The calculated rate constants $k(v=0, T)$ and $k(v=1, T)$ are displayed graphically in an Arrhenius plot in Figure 4, and selected points are listed in Table III. [From now on $k(v=0, T)$ will be simply designated as k , and $k(v=1, T)$ will be designated k^\dagger .] In the temperature range 298-1000°K these rates are fit very well by the nonlinear Arrhenius formulas

$$k = 2.81T \times 10^{-14} \exp(-4279/T) \quad (7)$$

and

Table III
Computed Results at Selected Temperatures

T	k	k^\dagger	k^\dagger/k	Γ
298	4.9 (-18) ^a	2.7 (-14) ^a	5465	4.4
300	5.4 (-18)	2.8 (-14)	5173	4.4
320	1.4 (-17)	4.4 (-14)	3107	4.2
350	4.8 (-17)	7.8 (-14)	1617	4.0
400	2.5 (-16)	1.7 (-13)	680	3.7
450	9.3 (-16)	3.2 (-13)	348	3.6
500	2.7 (-15)	5.5 (-13)	204	3.4
700	4.3 (-14)	2.3 (-12)	52	3.0
1000	3.9 (-13)	7.3 (-12)	19	2.8

^aThe units of k and k^\dagger are $\text{cm}^3 \text{ molecule}^{-1} \text{ sec}^{-1}$. The number in parenthesis is the power of 10.

$$k^{\dagger} = 4.65T \times 10^{-14} \exp(-1868/T) \quad (8)$$

where the units are $\text{cm}^3 \text{ molecule}^{-1} \text{ sec}^{-1}$.

Birely et al.¹ have set an upper bound on k^{\dagger} of $10^{-13} \text{ cm}^3 \text{ molecule}^{-1} \text{ sec}^{-1}$ at 300°K . Our value at this temperature is $2.8 \times 10^{-14} \text{ cm}^3 \text{ molecule}^{-1} \text{ sec}^{-1}$. This upper bound is 3.6 times larger than our computed value. Birely has also set an upper bound on the ratio; $k^{\dagger}/k \leq 3.8 \times 10^4$. Our value for this ratio at 300°K is $k^{\dagger}/k = 5.2 \times 10^3$. Birely's ratio was calculated using the extrapolated Leeds data¹³ for his value of k at 300°K , whereas our results are computed using the higher calculated value of k at this temperature. Values of our computed ratio at selected temperatures are listed in Table III. A good fit is given by the formula

$$k^{\dagger}/k = 1.65 \exp(2411/T) \quad (9)$$

The branching ratio Γ was calculated for the case in which H_2 is initially in the $v = 1$ state. This quantity is by definition equal to ratio of the state-to-state rate constants, $k(v=1, v'=1; T)/k(v=1, v'=0; T)$. These rate constants were evaluated by the same method used previously, i.e., the computed state-to-state cross sections $\sigma_0(v, J, v'; E)$ were fit to the function (5), then the rates were evaluated by integrating Eq. (3) with $\sigma(v, J; E)$ replaced by $\sigma_0(v, J, v'; E)$. Branching ratio values at selected temperatures are listed in Table III. These points can be fit quite well to the formula

$$\Gamma = 2.3 \exp(196/T) \quad (10)$$

The value of the branching ratio is sensitive to the method used to determine the final vibration quantum number v' . The method used in these calculations is the quasiclassical trajectory histogram method in which $v' + 1/2$ is calculated^{16a} as a continuous variable and then rounded to the nearest integer. This could probably be improved on by

using the recently proposed methods of Truhlar and Duff²¹ and of Bowman and Leasure.²²

Experiments are in progress⁹ to measure the rate k^\dagger and the branching ratio Γ at 300°K. The results are still being analyzed, so we cannot yet give a comparison of calculated and experimental values.

A great number of experimental measurements of k by a variety of methods and over a wide temperature range have been carried out.^{12,13,23} From an evaluation of selected high and low temperature measurements, the Leeds group (Baulch et al.)¹³ have recommended the expression $k = 3 \times 10^{-14} \text{ Texp}(-4480/T) \text{ cm}^3 \text{ molecule}^{-1} \text{ sec}^{-1}$ in the temperature range 400-2000°K. Several authors^{12,23} have recently expressed the opinion that this formula does not show quite enough curvature; in particular, it underestimates the rate at low temperatures. It is plotted as the dashed curve in Figure 4. Our calculated results lie above on the solid curve labeled $v = 0$. The Campbell and Thrush point is also plotted in this figure. At 500°K the calculated k is larger than the Leeds value by a factor of 1.4 and at 1000°K the factor is 1.15.

The greatest source of uncertainty in the reliability of the calculated results is our lack of detailed information about the potential surface. Our choice of the simple LEPS function is a first approximation consistent with our limited knowledge of the interatomic potential. At the present time we have no good reason for choosing any other potential; however, it is useful to have some idea of the effect that certain changes in the shape of the potential can have on the computed rates.

The extended LEPS function²⁴ is a more flexible surface with three adjustable (Sato) parameters. Two of these parameters will be equal due to the symmetry of the potential with respect to interchanging the hydrogen atoms. This leaves two quantities to adjust which allows us, within certain limits, to control both the position and height of the energy barrier independently. The effect of changing the barrier position was studied by Polanyi et al.²⁵⁻²⁷ Their results show that for

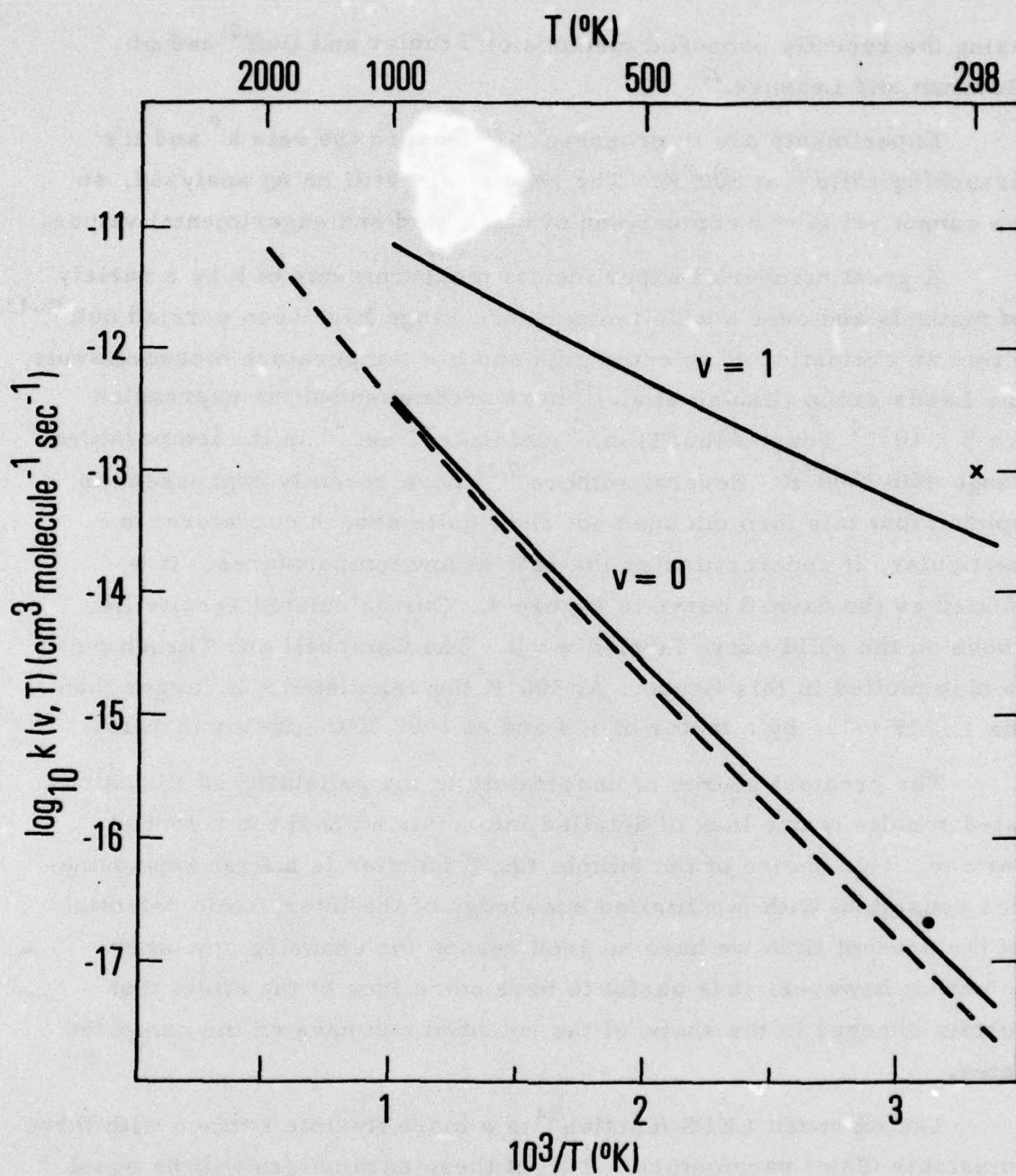


Figure 4. Rate constants, $k(v, T)$, for the reaction $O + H_2(v) \rightarrow OH + H$ where v is the vibrational quantum number of H_2 . The dashed line is a plot of the rate $k = 3.0 \times 10^{-14} T \exp(-4480/T)$, recommended by the Leeds group.¹³ Also shown are the experimental rate (●) of Campbell and Thrush¹¹ and the experimental upper bound (X) established by Birely et al.¹

endothermic reactions, moving the barrier into the exit valley of the potential surface increased the effectiveness of the vibrational energy in promoting reactions. In a preliminary set of calculations we verified these general conclusions for this reaction. The Sato parameters of the extended LEPS surface were adjusted (to $\Delta_{\text{OH}} = 0.14$ and $\Delta_{\text{HH}} = 0.03025$) so that the barrier height was the same (12.5 kcal/mole) but moved further into the exit valley (O-H = 1.07Å and H-H = 1.03Å compared to O-H = 1.12 and H-H = 0.95 in our original surface). The results showed a small increase in the $v = 0$ reactive cross sections (about 10 percent for $J = 1$ at 10 kcal/mole) and a rather substantial increase in the $v = 1$ reactive cross section (about 300 percent for $J = 1$ at 6 kcal/mole) along with a lowering of the threshold energy. Several other cross sections were also calculated with results of a similar order. The conclusion is that both k and k^\dagger increase as the barrier moves into the exit valley with the change in k^\dagger large compared to the change in k .

Clearly, further work is required, especially with regard to the potential surface. An ab-initio calculation of the $\text{O} + \text{H}_2$ reaction surface²⁸ indicates the barrier position is slightly more into the reactant channel (O-H = 1.15Å and H-H = 0.85Å) than the LEPS surface used here. This would tend to diminish the vibrational acceleration. In order to more accurately determine this effect, we anticipate carrying out a new set of trajectory calculations using the ab-initio surface when it is completed.

References

1. J. H. Birely, J. V. V. Kasper, F. Hai and L. A. Darnton, Chem. Phys. Lett. 31, 220 (1975).
2. J. H. Birely, J. Photo. Chem. 4, 269 (1975).
3. V. S. Letokhov, Science 180, 451 (1973).
4. W. Braun, M. J. Kurylo, A. Kalder and R. P. Wayne, J. Chem. Phys. 61, 461 (1974).
5. A. Kalder, W. Braun and M. J. Kurylo, J. Chem. Phys. 61, 2496 (1974).
6. M. J. Kurylo, W. Braun, C. N. Zaun and A. Kalder, J. Chem. Phys. 62, 2065 (1975).
7. J. C. Polyanyi, Faraday Discussions Chem. Soc. 55, 389 (1973).
8. R. F. Heidner, III and J. V. V. Kasper, Chem. Phys. Lett. 15, 179 (1972).
9. G. C. Light, personal communication.
10. See reference 16a for the functional form of the LEPS surface, also see reference 24 for a discussion and references concerning this function.
11. I. M. Campbell and B. A. Thrush, Trans. Faraday Soc. 64, 1265 (1968).
12. R. N. Dubinsky and D. J. McKenney, Can. J. Chem. 53, 3531 (1975).
13. D. L. Baulch, D. D. Drysdale, D. G. Horne and A. C. Lloyd, "Evaluated Kinetic Data for High Temperature Reactions, Volume 1, Homogeneous Gas Phase Reactions of the H_2-O_2 Systems," (Butterworths, London, 1972).
14. CLASTR was written by J. T. Muckerman and obtained from the Quantum Chemistry Program Exchange. This program is based on the theoretical analysis of Karplus, Porter and Sharma¹⁵ with additional details given by Muckerman.¹⁶
15. M. Karplus, R. N. Porter and R. D. Sharma, J. Chem. Phys. 43, 3259 (1965).

16. (a) J. T. Muckerman, J. Chem. Phys. 54, 1155 (1971);
(b) *ibid.* 56, 2997 (1972);
(c) *ibid.* 57, 3388 (1972).
17. The procedure we followed was suggested in unpublished class notes (1972) by R. N. Porter. For somewhat similar procedures see also L. M. Raff, D. L. Thompson, L. B. Sims and R. N. Porter, J. Chem. Phys. 56, 5998 (1972); R. N. Porter, L. B. Sims, D. L. Thompson and L. M. Raff, *ibid.* 58, 2855 (1973); R. N. Porter, D. L. Thompson, L. M. Raff and J. M. White, *ibid.* 62, 2429 (1975).
18. D. G. Truhlar, J. Chem. Phys. 56, 3189 (1972).
19. J. T. Muckerman and M. D. Newton, J. Chem. Phys. 56, 3191 (1972).
20. A. A. Westenberg and N. de Haas, J. Chem. Phys. 47, 4241 (1967).
21. D. G. Truhlar and J. W. Duff, Chem. Phys. Lett. 36, 551 (1975).
22. J. M. Bowman and S. C. Leasure, "An Improved Quasicalssical Histogram Method," preprint.
23. G. L. Schott, R. W. Getzinger and W. A. Seitz, Inter. J. of Chem. Kinetics 9, 921 (1974).
24. P. F. Kuntz, E. M. Nemeth, J. C. Polanyi, S. D. Rosner and C. E. Young, J. Chem. Phys. 44, 1168 (1966).
25. J. C. Polanyi and W. H. Wong, J. Chem. Phys. 51, 1439 (1969).
26. B. A. Hodgson and J. C. Polanyi, J. Chem. Phys. 55, 4745 (1971).
27. D. S. Perry, J. C. Polanyi and C. Woodrow Wilson, Jr., Chem. Phys. 3, 317 (1974).
28. N. W. Winter, unpublished results.

THE IVAN A. GETTING LABORATORIES

The Laboratory Operations of The Aerospace Corporation is conducting experimental and theoretical investigations necessary for the evaluation and application of scientific advances to new military concepts and systems. Versatility and flexibility have been developed to a high degree by the laboratory personnel in dealing with the many problems encountered in the nation's rapidly developing space and missile systems. Expertise in the latest scientific developments is vital to the accomplishment of tasks related to these problems. The laboratories that contribute to this research are:

Aerophysics Laboratory: Launch and reentry aerodynamics, heat transfer, reentry physics, chemical kinetics, structural mechanics, flight dynamics, atmospheric pollution, and high-power gas lasers.

Chemistry and Physics Laboratory: Atmospheric reactions and atmospheric optics, chemical reactions in polluted atmospheres, chemical reactions of excited species in rocket plumes, chemical thermodynamics, plasma and laser-induced reactions, laser chemistry, propulsion chemistry, space vacuum and radiation effects on materials, lubrication and surface phenomena, photo-sensitive materials and sensors, high precision laser ranging, and the application of physics and chemistry to problems of law enforcement and biomedicine.

Electronics Research Laboratory: Electromagnetic theory, devices, and propagation phenomena, including plasma electromagnetics; quantum electronics, lasers, and electro-optics; communication sciences, applied electronics, semiconducting, superconducting, and crystal device physics, optical and acoustical imaging; atmospheric pollution; millimeter wave and far-infrared technology.

Materials Sciences Laboratory: Development of new materials; metal matrix composites and new forms of carbon; test and evaluation of graphite and ceramics in reentry; spacecraft materials and electronic components in nuclear weapons environment; application of fracture mechanics to stress corrosion and fatigue-induced fractures in structural metals.

Space Sciences Laboratory: Atmospheric and ionospheric physics, radiation from the atmosphere, density and composition of the atmosphere, aurorae and airglow; magnetospheric physics, cosmic rays, generation and propagation of plasma waves in the magnetosphere; solar physics, studies of solar magnetic fields; space astronomy, x-ray astronomy; the effects of nuclear explosions, magnetic storms, and solar activity on the earth's atmosphere, ionosphere, and magnetosphere; the effects of optical, electromagnetic, and particulate radiations in space on space systems.

THE AEROSPACE CORPORATION
El Segundo, California